Computers and Chemical Engineering 172 (2023) 108176

Contents lists available at ScienceDirect

Computers and Chemical Engineering

journal homepage: www.elsevier.com/locate/cace

Design of low-carbon multi-energy systems in the SecMOD framework by combining MILP optimization and life-cycle assessment

Christiane Reinert [a,1], Niklas Nolzen [a,c,1], Julia Frohmann [a], Dominik Tillmanns [a], André Bardow [a,b,c,*]

[a] Institute of Technical Thermodynamics, RWTH Aachen University, 52062 Aachen, Germany
[b] Institute of Energy and Climate Research, Energy Systems Engineering (IEK-10), Forschungszentrum Jülich GmbH, 52425 Jülich, Germany
[c] Energy & Process Engineering, Department of Mechanical and Process Engineering, ETH Zurich, 8092 Zurich, Switzerland

ARTICLE INFO

Dataset link: https://git-ce.rwth-aachen.de/ltt/secmod-milp, https://ecoinvent.org/

Keywords:
Mixed integer-linear program
Integrated assessment model
Energy transition
Pumped-thermal energy storage
Sector coupling
Utility system

ABSTRACT

Decarbonizing complex industrial energy systems is an important step to mitigate climate change. Designing the transition of such sector-coupled industrial energy systems to low-carbon designs is challenging since both cost-efficient operation and the reduction of environmental impacts over the whole life cycle need to be considered in the system design. Optimal system designs can be identified using software: Recently, the open-source framework SecMOD was introduced for the linear optimization of multi-energy system models, considering environmental impacts by fully integrating life-cycle assessment. In this work, we extend SecMOD to allow mixed-integer decisions that are vital to model industrial energy systems. Thereby, we provide the first open-source mixed-integer linear program framework with full integration of life-cycle assessment. We use SecMOD to investigate the benefits of a pumped-thermal energy storage system in a sector-coupled industrial energy system and identify trade-offs regarding the system design by comparing the economic and climate optimum.

1. Introduction

Climate change and the resulting political developments require industrial energy systems with low-carbon energy converters to reduce the carbon footprint and decrease dependency on fossil resources, such as natural gas. Hence, new energy system designs now increasingly aim to integrate low-carbon energy from renewable sources to reduce greenhouse gas emissions (Ringkjøb et al., 2018). While renewable energy is increasingly deployed in the electricity sector worldwide, its contribution to supply heat, e.g., by biomass, has stagnated (International Energy Agency, 2021). Sector-coupling may help to bridge this gap and lead to synergy effects between sectors, e.g., by power-to-heat processes using heat pumps (Guelpa et al., 2019).

In order to develop environmentally beneficial systems, new energy system designs need to ensure that environmental burdens are not shifted to other parts of the life cycle or to other environmental impacts.

The need to consider environmental aspects beyond climate change, volatile electricity supply of renewables, and sectoral interaction leads to highly complex and interconnected systems. Identifying the optimal energy system design is a challenge that can be best addressed by mathematical optimization (Andiappan, 2017). As mathematical optimization is a powerful but elaborate tool, in recent years, several frameworks for the optimization of energy systems have been published with a focus on reduced modeling effort and enhanced reusability (Ringkjøb et al., 2018; Lopion et al., 2018). A framework is a flexible software toolbox that can comprise data processing, generalized equations, and optimization procedures. Hence, the framework builds specific models that can be flexibly developed and optimized (Hilpert et al., 2018).

However, such frameworks usually focus, in particular, on energy systems at a large-scale and, thus, model the energy system with reduced mathematical complexity, usually as a linear program (LP), e.g., Sánchez Diéguez et al. (2022), EnergyScope TD (Limpens et al., 2019) or PyPSA (Brown et al., 2018). To facilitate the transition towards low-carbon energy supply, tools are necessary for optimizing industrial energy systems, which typically require the tool to account for mixed-integer decisions to model discrete components, including part-load behavior (Kantor et al., 2020). Software from commercial providers, such as Top-Energy (TOP-Energy, 2022) and the Siemens prototype tool mm.esd (Hoettecke et al., 2022), allows the modeling and optimization of the energy system to a high level of detail. However, such tools

* Corresponding author at: Energy & Process Engineering, Department of Mechanical and Process Engineering, ETH Zurich, 8092 Zurich, Switzerland.
E-mail address: abardow@ethz.ch (A. Bardow).
[1] Both authors contributed equally and earned the right to list their name on their CV first.

https://doi.org/10.1016/j.compchemeng.2023.108176
Received 28 October 2022; Received in revised form 30 January 2023; Accepted 11 February 2023
Available online 21 February 2023

Table 1
Overview of the features of the SecMOD MILP and SecMOD LP framework (Reinert et al., 2022b) compared to common energy system optimization models and frameworks. Some frameworks are presented in several publications with different model features. The listing in this table refers to the specific features in the publications cited here.

Features	SecMOD MILP	SecMOD LP	Hilpert et al. (2018)	Sánchez Diéguez et al. (2022)	Limpens et al. (2019)	Brown et al. (2018)	TOP-Energy (2022)	Hoettecke et al. (2022)	Fleschutz et al. (2022)	Langiu et al. (2021)
Continuous sizing of discrete components	✓		✓				✓	✓	✓	✓
Detailed modeling of component operation	✓		✓			(✓)	✓	✓	✓	✓
Life-cycle assessment	✓	✓								
Multi-objective optimization	✓	✓					✓		✓	✓
Multi-graph networks (spatial resolution)	✓	✓	✓	✓		✓				✓
Transition pathways incl. brownfield optimization	✓	✓		✓			✓	✓	(✓)	(✓)
Open-source available	✓	✓	✓		✓	✓			✓	✓

require commercial licenses thereby limiting accessibility and are usually not available in open source.

Pfenninger et al. (2018) highlight that reusability is limited when models are not openly available. Generalized and modular open-source software frameworks ensure reusability and, thus, contribute to accelerating transparent research. Recently, open-source frameworks have been developed for optimizing industrial energy systems with mixed-integer decisions. For example, the open-source Demand Response Analysis Framework (DRAF) (Fleschutz et al., 2022) optimizes the design and operation of industrial energy systems considering both costs and time-dependent greenhouse gas emissions in a multi-criteria optimization. The component-oriented modeling approach of the open-source framework COMANDO (Langiu et al., 2021) enables the consideration of non-linearities and parametric uncertainties. While both frameworks are open-source and are applicable to energy systems at an industrial scale, they do not allow for a holistic life-cycle assessment. While the available tools thus provide valuable insights for energy system planners, current frameworks lack a holistic approach to account for the environmental impacts over the whole life cycle within the energy system's design and operation (Cook et al., 2022).

Such a holistic approach to embody environmental impacts is needed: As the switch to renewable energy supply leads to a shift from direct emissions to infrastructure-related emissions (Reinert et al., 2021), decision-making should take into account environmental impacts over the whole life cycle. Hugo and Pistikopoulos (2005) and Gerber et al. (2013) therefore integrated MILP optimization and life-cycle assessment, demonstrating the importance of this holistic perspective. However, a flexibly adaptable and openly available framework is still missing for the integration of energy system optimization and life-cycle assessment.

For this purpose, the object-oriented framework SecMOD was recently published and considers energy conversion, transport, and storage (Reinert et al., 2022b). The SecMOD framework considers life-cycle assessment (as standardized in ISO, 2020a and ISO, 2020b) for a holistic assessment of the energy system. However, currently, SecMOD is limited to linear program (LP) optimization.

1.1. Contribution of this work

In this work, we extend SecMOD from LP to MILP, modifying SecMOD to account for integer decisions necessary to consider energy systems at an industrial scale. Thereby, our newly developed MILP version of SecMOD is used to model an industrial energy system with continuous sizing of discrete components: For the discrete production components, the MILP formulation introduces integer decisions to (1) model minimum part-load and (2) approximate the nonlinear part-load behavior as a piecewise-affine function, and (3) model operation for the discrete storage components. We extend our conference publication (Reinert et al., 2022a) by elaborating on the MILP extension in more detail and by providing SecMOD MILP as an open-source framework (Section 2).

We demonstrate the capabilities of the SecMOD MILP framework by analyzing pumped-thermal energy storage (PTES) in a low-carbon industrial energy system (Section 3). PTES systems can strengthen sector-coupling by addressing volatility in electricity supply to provide electricity and heat flexibly (Dumont et al., 2020): During high feed-in of renewable electricity, PTES systems convert electricity into heat and store the heat that cannot be immediately used. Later, the stored heat can either fulfill a heat demand or be re-converted to electricity. If the used electricity is from renewable sources, PTES systems can contribute to a secure and low-carbon energy supply. Finally, we provide the conclusions (Section 4).

2. Method: Combining MILP optimization and life-cycle assessment

We extend the linear program (LP) formulation of the SecMOD framework (Reinert et al., 2022b) to a mixed-integer linear program (MILP) formulation. Table 1 gives an overview of the features to show the capabilities of both formulations compared to common energy system optimization models and frameworks. The MILP formulation allows for the optimization of industrial energy systems based on a user-defined superstructure (Voll et al., 2013). Within the superstructure-based optimization, the MILP formulation can consider continuous sizing of discrete production and storage components and integer decisions during operation, e.g., to model part-load behavior (Kämper et al., 2021b). Thus, the optimization decides on the installation of components, their optimal size, and how the selected components are operated to supply the user-defined demands.

While integer variables are required to model the minimum part load, the part-load behavior could also be modeled nonlinearly. However, the resulting MINLPs are difficult to solve for global optimality (Mitsos et al., 2018). Recent publications highlight that piecewise-affine approximations yield sufficient results and computation times while guaranteeing global optima with commercially available solvers (Kotzur et al., 2021; Kämper et al., 2021a).

By integrating a life-cycle assessment, different objective functions can be considered in a single or multi-objective optimization. Hence, the framework can find both cost-optimal and environmentally optimal solutions to explore trade-offs. Both LP SecMOD and MILP SecMOD offer features, such as multi-graph networks to account for spatial resolution, transition pathways, and brownfield optimization. Fig. 1 shows the optimization workflow within the SecMOD MILP framework.

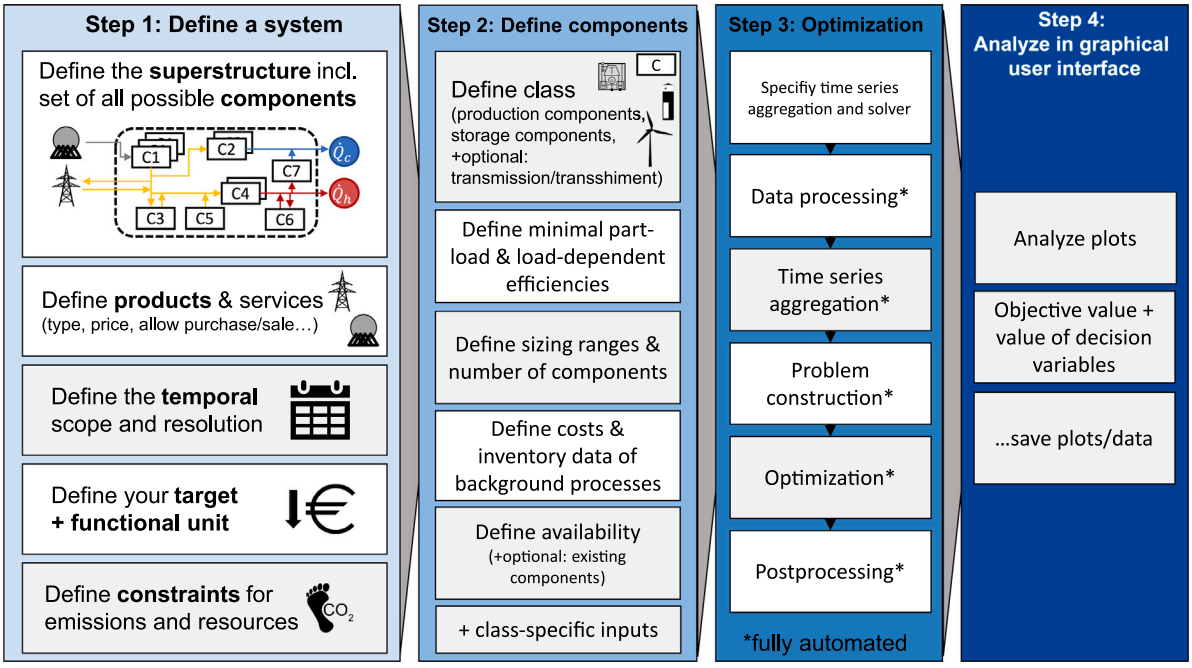

Fig. 1. Workflow for using the SecMOD MILP framework, extending the workflow of SecMOD LP (Reinert et al., 2022b): In the first step, the user defines a system, including the superstructure. In the second step, the components within the superstructure are defined. Subsequently, the optimization is performed. Last, the obtained results can be analyzed in a graphical user interface.

Thereby, the SecMOD MILP formulation provides an open-source framework that is able to optimize the design and operation of industrial energy systems. The framework, including the entire equations and all features, is published open-source at https://git-ce.rwth-aachen.de/ltt/secmod-milp. The modular structure allows the flexible consideration of the features mentioned above, depending on the user settings. In the following subsections, we present the extensions compared to the LP SecMOD formulation by Reinert et al. (2022b). For a description of the remaining feature set, we refer to the paper of Reinert et al. (2022b) and the open-source git-repository.

Section 2.1 explains the decision setting for industrial energy systems by introducing the problem statement. Subsequently, we present the flexible objection function and limits on expenditures in Section 2.1.1 that allow us to set up a multi-criteria optimization. Section 2.1.2 presents the product balance for the multi-energy system. Afterward, we present the extensions of the SecMOD MILP formulation compared to Reinert et al. (2022b). Sections 2.2 and 2.3 show the constraints that model discrete production components and storage components, emphasizing the need for binary variables.

2.1. Problem statement

The SecMOD MILP formulation optimizes the design and operation of an industrial energy system (cf. Fig. 1). The industrial energy system supplies pre-defined demands of products $b \in B$ (e.g., electricity, heat, etc.) in time steps $t \in T$. In the framework, the user defines a superstructure consisting of production components $c \in C^{\text{prod}}$ and storage components $c \in C^{\text{stor}}$. The superstructure represents all possibilities for the design of the industrial energy system.

Given the user-defined superstructure, the optimization aims to find the optimal design and operation of the industrial energy system for the objective function specified by the impact $imp \in IMP$. Here, the impacts can be either cost or environmental impacts. The optimization determines the design, including the continuous sizing of discrete production and storage components. For this purpose, we introduce the binary variables $Z^{\text{prod,part}}_{c,s,t}$ for production components and $Z^{\text{stor,exist}}_{c}$ for storage components. The optimized system consists of production components with capacity $P^{\text{prod,nom}}_{c}$ and storage components with capacity $P^{\text{stor,nom}}_{c}$. Depending on the desired optimization, SecMOD requires initial values for none of the capacities (Greenfield optimization), some of the capacities (Brownfield optimization), and all of the capacities (Operational optimization).

In each time step $t \in T$, the product demand is covered by the energy flows $P^{\text{prod,load}}_{c,s,t}$ from the production components, and the energy flows from charging $P^{\text{stor,load,in}}_{b,c,t}$ or discharging $P^{\text{stor,load,out}}_{b,c,t}$ the storage components. Therein, the binary variables $Z^{\text{stor,in}}_{c,t}$ and $Z^{\text{stor,out}}_{c,t}$ restrict the storage operation per time step to allow either charging or discharging the storage component. Additionally, products can be purchased $P^{\text{buy}}_{b,t}$ (e.g. natural gas) or sold $P^{\text{sell}}_{b,t}$ (e.g. electricity) externally in each time step $t \in T$. If desired, the user can forbid the purchase and sale of specific products, e.g., to model stand-alone systems.

2.1.1. Objective function and expenditure limits

We formulate the SecMOD MILP as a multi-criteria optimization with a flexible objective function. The consideration of different impacts $imp \in IMP$ in the objective function allows the exploration of optimal solutions in a single or multi-objective optimization. In addition, Pareto curves can be obtained with the epsilon-constrained method by adjusting the expenditure limits in Eqs. (2)–(4).

The objective function minimizes the total annual expenditures for a user-defined impact imp as

$$
\begin{aligned}
\min \; & \underbrace{\sum_{c \in C^{\text{prod}}} \frac{\mathrm{k}^{\text{inv,prod}}_{c,imp}}{\mathrm{pvf}_c} \cdot P^{\text{prod,nom}}_{c} + \sum_{c \in C^{\text{stor}}} \frac{\mathrm{k}^{\text{inv,stor}}_{c,imp}}{\mathrm{pvf}_c} \cdot P^{\text{stor,nom}}_{c}}_{CAPEX_{imp}} \\
& + \underbrace{\sum_{c \in C^{\text{prod}}} \sum_{t \in T} \sum_{s \in S} \mathrm{k}^{\text{op,prod}}_{c,imp} \cdot P^{\text{prod,load}}_{c,s,t} \cdot \Delta \mathrm{t}_t}_{OPEX^{\text{prod}}_{imp}} \\
& + \underbrace{\sum_{b \in B} \sum_{c \in C^{\text{stor}}} \sum_{t \in T} \mathrm{k}^{\text{op,stor}}_{c,imp} \cdot (P^{\text{stor,load,in}}_{b,c,t} + P^{\text{stor,load,out}}_{b,c,t}) \cdot \Delta \mathrm{t}_t}_{OPEX^{\text{stor}}_{imp}} \\
& + \underbrace{\sum_{b \in B} \sum_{t \in T} \mathrm{k}^{\text{buy}}_{b,t,imp} \cdot P^{\text{buy}}_{b,t} \cdot \Delta \mathrm{t}_t - \sum_{b \in B} \sum_{t \in T} \mathrm{k}^{\text{sell}}_{b,t,imp} \cdot P^{\text{sell}}_{b,t} \cdot \Delta \mathrm{t}_t}_{OPEX^{\text{exchange}}_{imp}} .
\end{aligned}
\tag{1}
$$

The total expenditures comprise annualized capital expenditures $CAPEX_{imp}$ and operational expenditures for production components $OPEX^{\text{prod}}_{imp}$, storage components $OPEX^{\text{stor}}_{imp}$, and the purchase and sale of products $OPEX^{\text{exchange}}_{imp}$. Depending on the user-selected impact imp, the expenditures can either consider cost or environmental impacts. For this purpose, the components in the superstructure require economic information (e.g., investment costs, maintenance costs), technical information (e.g., lifetime, load-dependent efficiencies), and environmental information. The environmental assessment requires a Life Cycle Inventory (LCI) for each component that can, e.g., be modeled in SecMOD via a combination of aggregated processes from ecoinvent. For a detailed list of the required inputs, including examples, we refer to the publication by Reinert et al. (2022b).

The capital expenditures $CAPEX$ arise from the installation of discrete production components $c \in C^{\text{prod}}$ sized with the nominal capacity $P^{\text{prod,nom}}_{c}$ and discrete storage components $c \in C^{\text{stor}}$ sized with the nominal capacity $P^{\text{stor,nom}}_{c}$. The specific investment costs for production components $\text{k}^{\text{inv,prod}}_{c,imp}$ and storage components $\text{k}^{\text{inv,stor}}_{c,imp}$ are annualized with the component-specific present value annuity factor pvf_c according to Broverman (2017), based on a user-defined interest rate. For capital expenditures, the specific annualized investment costs are multiplied by the respective nominal capacities.

The operational expenditures $OPEX$ arise from the operation of the production and storage components as well as from the purchase and sale of products $b \in B$ in each time step $t \in T$. In each time step $t \in T$, the operational expenditures consist of the specific operating costs of the production $\text{k}^{\text{op,prod}}_{c,imp}$ and storage components $\text{k}^{\text{op,stor}}_{c,imp}$, multiplied by the load of the production components $P^{\text{prod,load}}_{c,s,t}$ and storage components $P^{\text{stor,load,in}}_{b,c,t}$ and $P^{\text{stor,load,out}}_{b,c,t}$. Storage components, therefore, can incur operating costs both during charging and discharging. For each product $b \in B$ and in each time step $t \in T$, the industrial energy system can purchase the product quantity $P^{\text{buy}}_{b,t}$ at specific cost $\text{k}^{\text{buy}}_{b,t,imp}$. In addition, the industrial energy system can sell the product quantity $P^{\text{sell}}_{b,t}$ at specific cost $\text{k}^{\text{sell}}_{b,t,imp}$. The sale of products results in a credit in the objective function. Ultimately, the operational expenditures of each time step t are multiplied by the time step duration Δt_t. The time step duration Δt_t indicates the length of the respective time step in hours.

Optionally, in SecMOD MILP, the user can restrict impacts imp resulting from the construction and the operation of the industrial energy system by

$$CAPEX_{imp} \leq \text{capex}^{\text{lim}}_{imp}, \tag{2}$$

$$OPEX^{\text{prod}}_{imp} + OPEX^{\text{stor}}_{imp} + OPEX^{\text{exchange}}_{imp} \leq \text{opex}^{\text{lim}}_{imp}, \tag{3}$$

$$CAPEX_{imp} + OPEX^{\text{prod}}_{imp} + OPEX^{\text{stor}}_{imp} + OPEX^{\text{exchange}}_{imp} \leq \text{totex}^{\text{lim}}_{imp}. \tag{4}$$

For each impact $imp \in IMP$, Eq. (2) limits the capital expenditures to $\text{capex}^{\text{lim}}_{imp}$, Eq. (3) limits the operational expenditures to $\text{opex}^{\text{lim}}_{imp}$, and Eq. (4) limits the total expenditures to $\text{totex}^{\text{lim}}_{imp}$.

It is possible to change the environmental impacts that are considered in the objective function and in the constraints. Furthermore, the user can change the environmental impacts associated with constructing or operating a component. In our work, we implemented ecoinvent to assess environmental impacts, as ecoinvent is the most commonly used database. In principle, any database can be integrated into SecMOD to assess the environmental impacts. However, minor modifications might be necessary. For the life cycle impact assessment, various impact assessment methods can be chosen.

2.1.2. Product balance

In the SecMOD MILP extension, the user can determine the purchase (e.g., gas) and sale (e.g., electricity) of products on an individual basis across the defined system boundary. If desired, the product demand for certain products can only be covered on-site (e.g., for heat), as the purchase and sale of specific products can be prohibited. Additionally, the user may allow on-site overproduction for some products.

The industrial energy system covers an exogenous product demand $\text{d}_{b,t}$ for each product $b \in B$ in each time step $t \in T$ with

$$\sum_{c \in C^{\text{prod}}} P^{\text{prod}}_{b,c,t} + \sum_{c \in C^{\text{stor}}} (P^{\text{stor,load,out}}_{b,c,t} - P^{\text{stor,load,in}}_{b,c,t}) + P^{\text{buy}}_{b,t} = \text{d}_{b,t} + P^{\text{sell}}_{b,t} \quad \forall\, b \in B, t \in T. \tag{5}$$

The exogenous demand $\text{d}_{b,t}$ can be covered by the operation of production and storage components. Here, the production $P^{\text{prod}}_{b,c,t}$ of production component $c \in C^{\text{prod}}$ in time step t is positive if the product b is produced or negative if a product b is consumed. Storage components $c \in C^{\text{stor}}$ can shift the product demand for product b in time by charging $P^{\text{stor,load,in}}_{b,c,t}$ or discharging $P^{\text{stor,load,out}}_{b,c,t}$ the storage components in time step t. In addition, the sale $P^{\text{sell}}_{b,t}$ and purchase $P^{\text{buy}}_{b,t}$ of products increases or decreases the exogenous demand.

2.2. Production components

Production components $c \in C^{\text{prod}}$ convert one or several input products $b \in B$ into one or several output products $b' \in B$. In the SecMOD MILP extension, we consider the installation of discrete production components. In case the production component is installed, the component can be sized within a predefined sizing range. To account for economies of scale, the user can define different sizing ranges for the respective production components in the superstructure with varying specific investment costs.

The operation of the installed production components considers part-load behavior, comprising minimal part load and load-dependent efficiencies for converting the inputs into the outputs. The conversion efficiency is approximated as a piecewise-affine linear function to avoid nonlinearities. Thus, part-load behavior is modeled as piecewise-affine linearization with $s \in S$ part-load segments that are scaled with the installed capacity $P^{\text{prod,nom}}_{c}$.

Eqs. (6)–(9) model the discrete construction and continuous sizing of production components within the minimal possible capacity $\text{cap}^{\text{prod,min}}_{c}$ and maximal possible capacity $\text{cap}^{\text{prod,max}}_{c}$, thus determining the installed capacity $P^{\text{prod,nom}}_{c}$ of the production component $c \in C^{\text{prod}}$. For this purpose, we adapt the equations from Voll et al. (2013) that employ the linearization from Glover (1975) leading to

$$\tilde{P}^{\text{prod,nom}}_{c,s,t} \leq Z^{\text{prod,part}}_{c,s,t} \cdot \text{cap}^{\text{prod,max}}_{c} \quad \forall\, c \in C^{\text{prod}}, s \in S, t \in T, \tag{6}$$

$$\tilde{P}^{\text{prod,nom}}_{c,s,t} \geq Z^{\text{prod,part}}_{c,s,t} \cdot \text{cap}^{\text{prod,min}}_{c} \quad \forall\, c \in C^{\text{prod}}, s \in S, t \in T, \tag{7}$$

$$\tilde{P}^{\text{prod,nom}}_{c,s,t} \leq P^{\text{prod,nom}}_{c} \quad \forall\, c \in C^{\text{prod}}, s \in S, t \in T, \tag{8}$$

$$\tilde{P}^{\text{prod,nom}}_{c,s,t} \geq P^{\text{prod,nom}}_{c} + (Z^{\text{prod,part}}_{c,s,t} - 1) \cdot \text{cap}^{\text{prod,max}}_{c} \quad \forall\, c \in C^{\text{prod}}, s \in S, t \in T. \tag{9}$$

For each production component, the sizing decision is coupled with the operation, since the installed capacity scales the piecewise-affine linearization of the part-load behavior. In Eqs. (6)–(9), we introduce the auxiliary capacity $\tilde{P}^{\text{prod,nom}}_{c,s,t}$ and the binary variable $Z^{\text{prod,part}}_{c,s,t}$. The binary variable $Z^{\text{prod,part}}_{c,s,t}$ equals one if the part-load segment s is active for production component c in time step t. The auxiliary capacity $\tilde{P}^{\text{prod,nom}}_{c,s,t}$ is equal to the capacity $P^{\text{prod,nom}}_{c}$ for the active part-load segment and scales the piecewise-affine linearization of the part-load behavior. Thus, for the active part-load segment, Eqs. (6)–(9) ensure that the auxiliary capacity $\tilde{P}^{\text{prod,nom}}_{c,s,t}$ equals the production capacity $P^{\text{prod,nom}}_{c}$. Otherwise, $Z^{\text{prod,part}}_{c,s,t}$ as well as $\tilde{P}^{\text{prod,nom}}_{c,s,t}$ are zero.

Finally, Eq. (10) ensures that at most one part-load segment is active for production component c and time step t:

$$\sum_{s \in S} Z^{\text{prod,part}}_{c,s,t} \leq 1 \quad \forall\, c \in C^{\text{prod}}, t \in T. \tag{10}$$

Eqs. (11)–(13) model the part-load behavior as piecewise-affine linearization. Exemplary, Fig. 2 shows the modeling of the part-load behavior for boiler B1, which converts natural gas into heat. The boiler B1

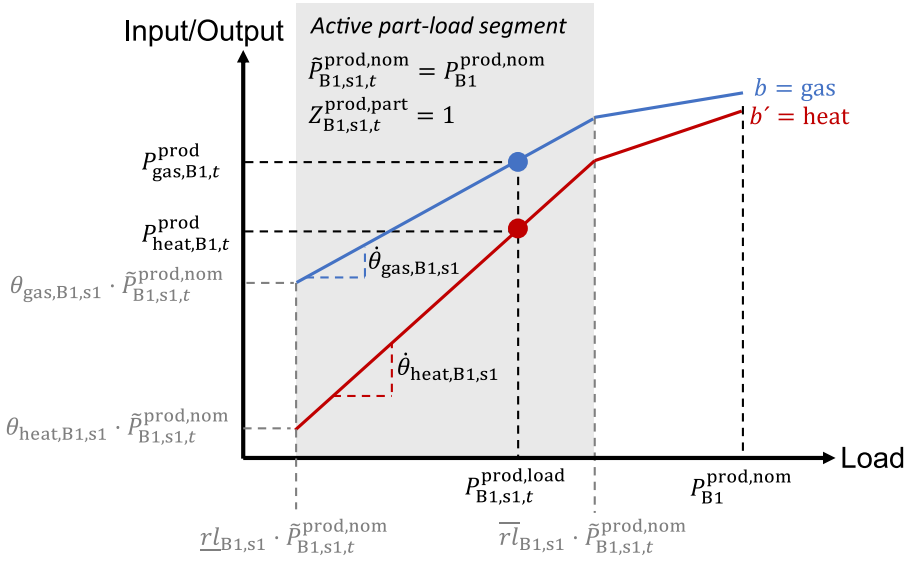

Fig. 2. Exemplary relation between the decision variables for a boiler B1 operated in the part-load segment s1. The decision variables are the capacity $P^{\text{prod,nom}}_{\text{B1}}$, the load $P^{\text{prod,load}}_{\text{B1,s1},t}$ and the input/output $P^{\text{prod}}_{\text{gas,B1},t}$ / $P^{\text{prod}}_{\text{heat,B1},t}$. The auxiliary capacity $\tilde{P}^{\text{prod,nom}}_{\text{B1,s1},t}$ equals the capacity $P^{\text{prod,nom}}_{\text{B1}}$ for the active part-load segment ($Z^{\text{prod,part}}_{\text{B1,s1},t}$) and scales the piecewise-affine linearization of the part-load behavior.

has the capacity $P^{\text{prod,nom}}_{\text{B1}}$ and is operated in part-load segment s1. In this case, the part-load segment s1 is set active since the binary variable $Z^{\text{prod,part}}_{\text{B1,s1},t}$ equals one. Based on the active part-load segment s1, the input/output $P^{\text{prod}}_{\text{gas,B1},t}$ / $P^{\text{prod}}_{\text{heat,B1},t}$ is determined depending on the load $P^{\text{prod,load}}_{\text{B1,s1},t}$. Therein, the minimal relative load $\underline{\text{rl}}_{\text{B1,s1}}$ and the maximum relative load $\overline{\text{rl}}_{\text{B1,s1}}$ multiplied by the auxiliary capacity $\tilde{P}^{\text{prod,nom}}_{\text{B1,s1},t}$ restrict the load $P^{\text{prod,load}}_{\text{B1,s1},t}$ to the active segment s1.

Eqs. (11)–(13) generalize the example from Fig. 2. For each production component $c \in C^{\text{prod}}$ and time step $t \in T$, Eq. (11) determines the input/output $P^{\text{prod}}_{b,c,t}$ depending on the load $P^{\text{prod,load}}_{c,s,t}$ as

$$P^{\text{prod}}_{b,c,t} = \sum_{s \in S} \underbrace{\theta_{b,c,s} \cdot \tilde{P}^{\text{prod,nom}}_{c,s,t}}_{\text{constant part}} + \underbrace{\dot{\theta}_{b,c,s} \cdot (P^{\text{prod,load}}_{c,s,t} - \underline{\text{rl}}_{c,s} \cdot \tilde{P}^{\text{prod,nom}}_{c,s,t})}_{\text{linear part}} \quad \forall b \in B, c \in C^{\text{prod}}, t \in T. \tag{11}$$

The right side of Eq. (11) accounts for the part-load behavior as piecewise-affine linearization with $s \in S$ part-load segments. For each part-load segment, the piecewise-affine linearization consists of two parts: a constant part modeling the minimal load and a linear part for the additional input/output along the segment. For the constant part, the multiplication of the parameter $\theta_{b,c,s}$ with the auxiliary capacity $\tilde{P}^{\text{prod,nom}}_{c,s,t}$ determines the input/output at the minimal load for the active part-load segment. For the linear part, the multiplication of the gradient $\dot{\theta}_{b,c,s}$ with the difference between the actual load $P^{\text{prod,load}}_{c,s,t}$ and the minimal load of the part-load segment determines the additional input/output along the segment. Note that the auxiliary capacity $\tilde{P}^{\text{prod,nom}}_{c,s,t}$ is 0 for all part-load segments that are not active. Thus, the sum over over all part-load segments yields the input/output $P^{\text{prod}}_{b,c,t}$, since only one part-load segment is active in each time step.

For production component c and in each time step t, Eqs. (12) and (13) restrict the load $P^{\text{prod,load}}_{c,s,t}$ to the minimum and maximum possible load within the part-load segment s

$$P^{\text{prod,load}}_{c,s,t} \leq \overline{\text{rl}}_{c,s} \cdot \tilde{P}^{\text{prod,nom}}_{c,s,t} \quad \forall c \in C^{\text{prod}}, s \in S, t \in T, \tag{12}$$

$$P^{\text{prod,load}}_{c,s,t} \geq \underline{\text{rl}}_{c,s} \cdot \tilde{P}^{\text{prod,nom}}_{c,s,t} \quad \forall c \in C^{\text{prod}}, s \in S, t \in T. \tag{13}$$

Therein, the load is restricted by multiplying the auxiliary capacity $\tilde{P}^{\text{prod,nom}}_{c,s,t}$ with the minimal relative load $\underline{\text{rl}}_{c,s}$ and the maximum relative load $\overline{\text{rl}}_{c,s}$.

Production components, such as wind turbines or photovoltaic systems, are not available at all or only partially available in some time steps t. The relative availability $\text{av}_{c,t}$, therefore, describes the share of usable capacity for each time step t and component c. The load $P^{\text{prod,load}}_{c,s,t}$ is then restricted by the usable production capacity with

$$P^{\text{prod,load}}_{c,s,t} \leq P^{\text{prod,nom}}_{c} \cdot \text{av}_{c,t} \quad \forall c \in C^{\text{prod}}, s \in S, t \in T. \tag{14}$$

The usable production capacity is determined for each production component c and time step t as the multiplication of the relative availability $\text{av}_{c,t}$ and the capacity $P^{\text{prod,nom}}_{c}$.

2.3. Storage components

This section presents the equations for the design, the sizing, and the operation of discrete storage components $c \in C^{\text{stor}}$. Storage components store a product $b \in B$ at time step $t \in T$ and discharge the product at a later time step, i.e., the storage component can either be charged or discharged in each time step. To allow either charging or discharging in each time step, the binary variables $Z^{\text{stor,in}}_{c,t}$ and $Z^{\text{stor,out}}_{c,t}$ are introduced to model the storage operation.

Eqs. (15) and (16) model the construction and sizing of a discrete storage component $c \in C^{\text{stor}}$ with

$$P^{\text{stor,nom}}_{c} \leq \text{cap}^{\text{stor,max}}_{c} \cdot Z^{\text{stor,exist}}_{c} \quad \forall c \in C^{\text{stor}}, \tag{15}$$

$$P^{\text{stor,nom}}_{c} \geq \text{cap}^{\text{stor,min}}_{c} \cdot Z^{\text{stor,exist}}_{c} \quad \forall c \in C^{\text{stor}}. \tag{16}$$

The binary variable $Z^{\text{stor,exist}}_{c}$ equals one if the storage c exists. In this case, the storage capacity $P^{\text{stor,nom}}_{c}$ is constrained between the minimum possible storage capacity $\text{cap}^{\text{stor,min}}_{c}$ and maximum possible storage capacity $\text{cap}^{\text{stor,max}}_{c}$. If the storage component c is not built, the binary variable $Z^{\text{stor,exist}}_{c}$ equals zero.

The storage capacity $P^{\text{stor,nom}}_{c}$ restricts the storage level $SL_{c,t}$ for all time steps $t \in T$ and storage components $c \in C^{\text{stor}}$ with

$$SL_{c,t} \leq P^{\text{stor,nom}}_{c} \quad \forall c \in C^{\text{stor}}, t \in T. \tag{17}$$

For some storage components (e.g., battery storage components), it is not possible to discharge the storage completely. Hence, Eq. (18) models the minimal storage level during operation

$$SL_{c,t} \geq P^{\text{stor,nom}}_{c} \cdot \text{sl}^{\text{stor,min}}_{c} \quad \forall c \in C^{\text{stor}}, t \in T. \tag{18}$$

For all time steps $t \in T$, the storage level $SL_{c,t}$ needs to be greater than the minimal usable storage capacity. The minimal usable storage

capacity is the minimal relative storage level $sl_c^{stor,min}$ multiplied with the storage capacity $P_c^{stor,nom}$ in Eq. (18).

The load variables $P_{b,c,t}^{stor,load,in}$ and $P_{b,c,t}^{stor,load,out}$ model the operation of the storage component. For each storage component c, the load variables specify the amount of product b charged or discharged in time step t. Depending on the load variables $P_{b,c,t}^{stor,load,in}$ and $P_{b,c,t}^{stor,load,out}$, Eq. (19) models the storage level $SL_{c,t}$ of each storage component $c \in C^{stor}$ for the product $b \in B$ as

$$SL_{c,t} \cdot (1 - \eta_c^{stor,loss}) + \Delta t_t (P_{b,c,t}^{stor,load,in} \cdot \eta_{b,c}^{stor,in} - P_{b,c,t}^{stor,load,out} \cdot \eta_{b,c}^{stor,out}) = SL_{c,t+1} \quad \forall b \in B, c \in C^{stor}, t \in T. \tag{19}$$

The storage level $SL_{c,t+1}$ in time step $t+1$ results from the storage level $SL_{c,t}$ in the previous time step t plus the charging load $P_{b,c,t}^{stor,load,in}$ and minus the discharging load $P_{b,c,t}^{stor,load,out}$ multiplied with the time step duration Δt_t. In Eq. (19), we consider charging and discharging losses by including the efficiencies $\eta_{b,c}^{stor,in}$ and $\eta_{b,c}^{stor,out}$. In addition, our modeling accounts for storage losses during a time step by including the relative storage efficiency $\eta_c^{stor,loss}$ in Eq. (19).

To reduce computational complexity, our framework includes clustering techniques that aggregate the time steps T to typical periods, e.g., typical days or typical weeks (Kotzur et al., 2018). For each of the typical periods, we consider closed and repeating cycles for the storage units. Thus, for an exemplary typical period, Eq. (20) links the storage level at the last time step t_{end} with the initial time step t0:

$$SL_{c,t_{end}} = SL_{c,t0} \quad \forall c \in C^{stor}. \tag{20}$$

Our storage modeling assumes a fixed ratio of storage load to storage capacity denoted by the parameter $pcr_{b,c}^{stor}$. Since the maximum storage load often scales with the storage capacity, Eqs. (21) and (22) restrict the load for charging $P_{b,c,t}^{stor,load,in}$ and discharging $P_{b,c,t}^{stor,load,out}$ as

$$P_{b,c,t}^{stor,load,in} \leq pcr_{b,c}^{stor} \cdot P_c^{stor,nom} \quad \forall b \in B, c \in C^{stor}, t \in T, \tag{21}$$

$$P_{b,c,t}^{stor,load,out} \leq pcr_{b,c}^{stor} \cdot P_c^{stor,nom} \quad \forall b \in B, c \in C^{stor}, t \in T. \tag{22}$$

For charging and discharging, the load is restricted to the storage load to storage capacity ratio $pcr_{b,c}^{stor}$ multiplied with the storage capacity $P_c^{stor,nom}$.

Finally, we introduce the binary variables $Z_{c,t}^{stor,in}$ and $Z_{c,t}^{stor,out}$ to model the storage operation. The binary variables equal one if the storage component c is charged and discharged in time step t, respectively, and zero otherwise. For each storage component $c \in C^{stor}$, Eq. (23) allows that either charging or discharging is possible in time step $t \in T$.

$$Z_{c,t}^{stor,in} + Z_{c,t}^{stor,out} \leq 1 \quad \forall c \in C^{stor}, t \in T. \tag{23}$$

Subsequently, the load is limited by the Big-M constraints Eqs. (24) and (25) with

$$P_{b,c,t}^{stor,load,in} \leq pcr_{b,c}^{stor} \cdot cap_c^{stor,max} \cdot Z_{c,t}^{stor,in} \quad \forall b \in B, c \in C^{stor}, t \in T, \tag{24}$$

$$P_{b,c,t}^{stor,load,out} \leq pcr_{b,c}^{stor} \cdot cap_c^{stor,max} \cdot Z_{c,t}^{stor,out} \quad \forall b \in B, c \in C^{stor}, t \in T. \tag{25}$$

The Big M is modeled as the multiplication of the power-to-capacity ratio $pcr_{b,c}^{stor}$ multiplied by the maximum possible storage size $cap_c^{stor,max}$.

Finally, the extensions presented in Section 2 allow the optimization and holistic assessment of industrial energy systems with discrete production and storage components. Thereby, the open-source SecMOD MILP framework provides a multi-objective optimization with a flexible objective function that allows us to find both cost-optimal and environmentally optimal solutions.

3. Case study: Integrating PTES in an industrial energy system design

In our case study, we demonstrate the capabilities of SecMOD MILP by capacity expansion planning in a sector-coupled industrial energy system. We optimize the system economically and environmentally in two scenarios with varying electricity and natural gas prices.

As discussed above, pumped-thermal energy storage (PTES) systems can strengthen sector-coupling by addressing volatility in electricity supply to flexibly provide both heat and electricity (Dumont et al., 2020). We, therefore, exploit the modular structure of SecMOD to include PTES as an emerging technology in the superstructure. Our study aims to examine the economic and environmental competitiveness of PTES in the industrial energy system under varying energy price scenarios for natural gas and electricity.

3.1. Superstructure of the industrial energy system

As a case study to evaluate the integration of the PTES, we examine a real-world industrial energy system located in Germany (Fig. 3), which was introduced by Voll et al. (2013) and extended by Baumgärtner et al. (2019). We expand the superstructure by adding low-carbon technologies (Baumgärtner et al., 2021), such as wind turbines, battery storage, and photovoltaics. Heat can be provided by combined heat and power units (CHP), natural gas boilers, or electric boilers. Cooling power is provided by absorption chillers or compression chillers, respectively. The superstructure of the industrial energy system consists of the components shown in Fig. 3.

The system is designed to satisfy temporally resolved electricity, heat, and cooling demands. In our adapted version, grid electricity and natural gas can be imported at specific costs and environmental impacts. Overproduction of electricity is allowed to occur at no costs or revenues to account for curtailment, while overproduction of heat or cooling is prohibited.

In addition, we further model a PTES system as an emerging technology. The PTES system consists of a high-temperature heat pump (based on Baumgärtner et al., 2021), sensible thermal storage with water as storage medium (Baumgärtner et al., 2019), and an organic Rankine cycle (ORC) (based on Stoppato and Benato, 2020, Tartière and Astolfi, 2017, and Tillmanns et al., 2022). The PTES can supply heat directly or feed the ORC for the reconversion to electricity, thereby adding flexibility across sectors.

Economies of scale during sizing are taken into account based on cost correlations by Baumgärtner et al. (2019) by allowing small, medium, and large components for the CHPs, chillers, and boilers. The components have different specific costs and part-load behavior. For all units, sizing can be chosen continuously between the minimum and maximum component sizes. Compared to a linear optimization problem, a MILP model can reflect component interaction that is influenced by part-load behavior. Part-load behavior and especially minimal part-load introduce additional restrictions to the energy system, such that some operation states are not possible in a MILP. These real-world features of energy systems lead, e.g., to the installation of redundant units (Voll et al., 2013). In comparison, a linear model, which neglects efficiency reductions due to part-load behavior and discrete component and operating limits, would underestimate the cost and climate change impact compared to the MILP. For a more detailed discussion about how model complexity impacts the results of design optimizations, please also refer to Wirtz et al. (2021).

We extend all component models with environmental models. Here, we employ the database ecoinvent 3.7.1 (Wernet et al., 2016). Each life cycle inventory (LCI) quantifies the material and energy flows needed to build and operate the component. We model the direct inputs and outputs of component operation using piecewise-affine linearization to reflect part-load efficiencies. The European Commission (Joint Research Center, 2010) recommends the determination of environmental

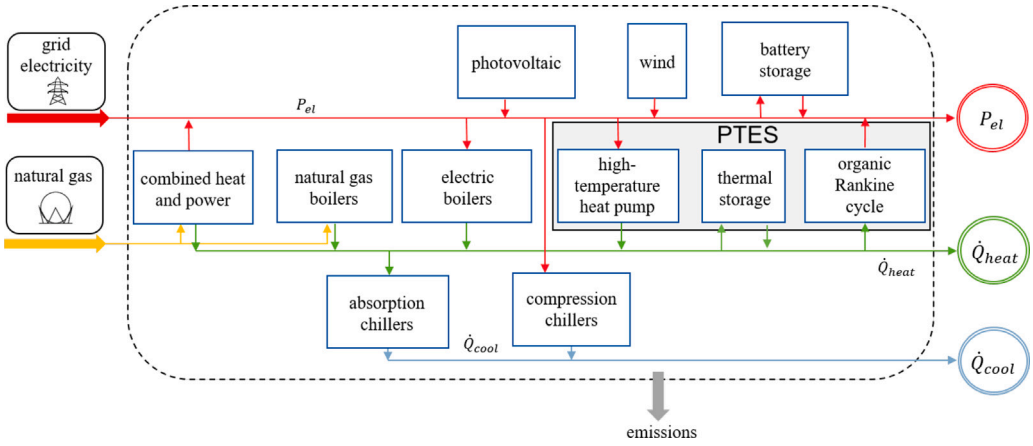

Fig. 3. Simplified superstructure of the utility system providing electricity (P_{el}), heating ($\dot{Q}_{heat}$), and cooling ($\dot{Q}_{cool}$) supply (extending on Voll et al., 2013). PTES is the pumped-thermal energy storage. For chillers and boilers, multiple units can be employed.

impacts using the Environmental Footprint methodology. This work focuses on the impact category "climate change" of Environmental Footprints 2.0, quantifying the global warming impact. We provide detailed information on the components in the Supporting Information.

We consider one year of operation, aggregated to six typical days with hourly resolution. Clustering is readily integrated into SecMOD. As a clustering technique for temporal aggregation, we use k-medoids (Kotzur et al., 2018). The economic objective function is the total annualized system cost. In this work, we consider an annualization horizon of 8 years and an interest rate of 5%.

In recent months, energy prices in Germany have changed rapidly, resulting in significantly altered costs for the operation of industrial energy systems. To quantitatively evaluate the implications of the price change on the optimal system design, we optimize two economic scenarios: Firstly, we consider a low-price scenario for natural gas (2.6 ct/kWh on average) and electricity (7.5 ct/kWh on average). Secondly, we consider a high-price scenario for natural gas (17.44 ct/kWh on average EEX Market Data Services, 2022) and electricity (26.64 ct/kWh on average BDEW, 2022). The price development changes the ratio of the electricity price to the gas price from 2.9 to 1.5, rendering electricity more favorable.

Thirdly, as an environmental objective, we minimize the annual climate impact. SecMOD allows us to consider environmental impacts either over parts of the life cycle or holistically over the whole life cycle. In our case study, the impacts from construction are annualized over the unit lifetime without discounting. The annual climate impact considers the whole life cycle of the system components.

Our model comprises 26 770 equations, 800 continuous variables, and 3746 binary variables after the presolve for the climate-optimal case. All other cases have a comparable number of equations, variables, and binary variables. All calculations are performed using 4 Intel-Xeon CPUs with 3.0 GHz and 64 GB RAM with Gurobi 9.0.0 and solved within a few minutes. Please note that in SecMOD, the optimization of larger problems is also possible. We terminate each optimization run when the optimality gap for each optimization reaches our termination criterion of one percent.

3.2. Results: economically and climate optimal energy supply structure

The scenarios show a trade-off between costs and climate impact (Fig. 4): While the cost-optimized system has the least cost in the low-price scenario, it also emits the most greenhouse gas emissions. In the high-price scenario, the cost increases by more than a factor of three, while the climate impact is reduced by more than half for the cost-optimal system. Thus, the high prices provide a strong incentive for decarbonization. The climate optimum is more than factor of 3.5 more expensive than the least-cost design with low energy prices. However, the cost of the climate optimum is not significantly higher than the cost of the high-price scenario. The climate impact is cut by around 80% compared to the low-price scenario.

The epsilon-constraint method generates Pareto frontiers that represent trade-offs in the multi-objective optimization. For each price scenario, we generated a Pareto frontier with five equidistant points. In SecMOD, other points of the Pareto frontier can also be calculated by manual selection to specifically adjust the resolution of the solution space. Future work could integrate advanced automated schemes to explore the Pareto frontier (cf. Mavrotas, 2009, Halffmann et al., 2022 and Petchrompo et al., 2022).

SecMOD can analyze in which phase of the life cycle emissions occur: While infrastructure-related emissions contribute merely by 2% to the overall climate impact in the cost-optimal system, infrastructure-related emissions are responsible for 85% of the overall climate impact in the climate-optimal scenario. Respectively, the role of infrastructure also increases when assessing system cost. Our results thus underline the need for a holistic assessment over the whole life cycle. Fig. 4 shows that operational emissions account for the major share of emissions in largely fossil-based systems. However, low-carbon energy systems require a more holistic approach.

Regarding further environmental impacts, which can be automatically assessed in SecMOD, we observe similar trends as in national energy systems (Baumgärtner et al., 2021; Reinert et al., 2021; Rauner and Budzinski, 2017): The low-carbon energy system leads to environmental co-benefits in most impact categories. For example, fossil resource depletion in the climate-optimal case is more than a factor of five lower than in the low-price cost optimum. However, the holistic approach of SecMOD also allows the detection of burden-shifting to other environmental impacts. In our case study, burden shifting leads to a significant increase in some impact categories, such as resource depletion of minerals and metals (by a factor of 2.2). SecMOD can be used to consider environmental impacts beyond climate change in the objective function and to limit them in constraints. Further research could analyze additional system designs by limiting other environmental impacts. For example, limiting the permissible increase in resource depletion of minerals and metals would likely move the solution towards less resource-intensive components.

Compared to the LP model, the MILP optimization allows a detailed analysis of the operational decisions for each component. Regarding the operational decisions, the cost-optimal system with low prices provides electricity predominantly by CHPs. Therefore, CHPs also provide the major share of heating. Furthermore, cooling is provided partly by the compression chillers and partly by the absorption chillers. Here, the

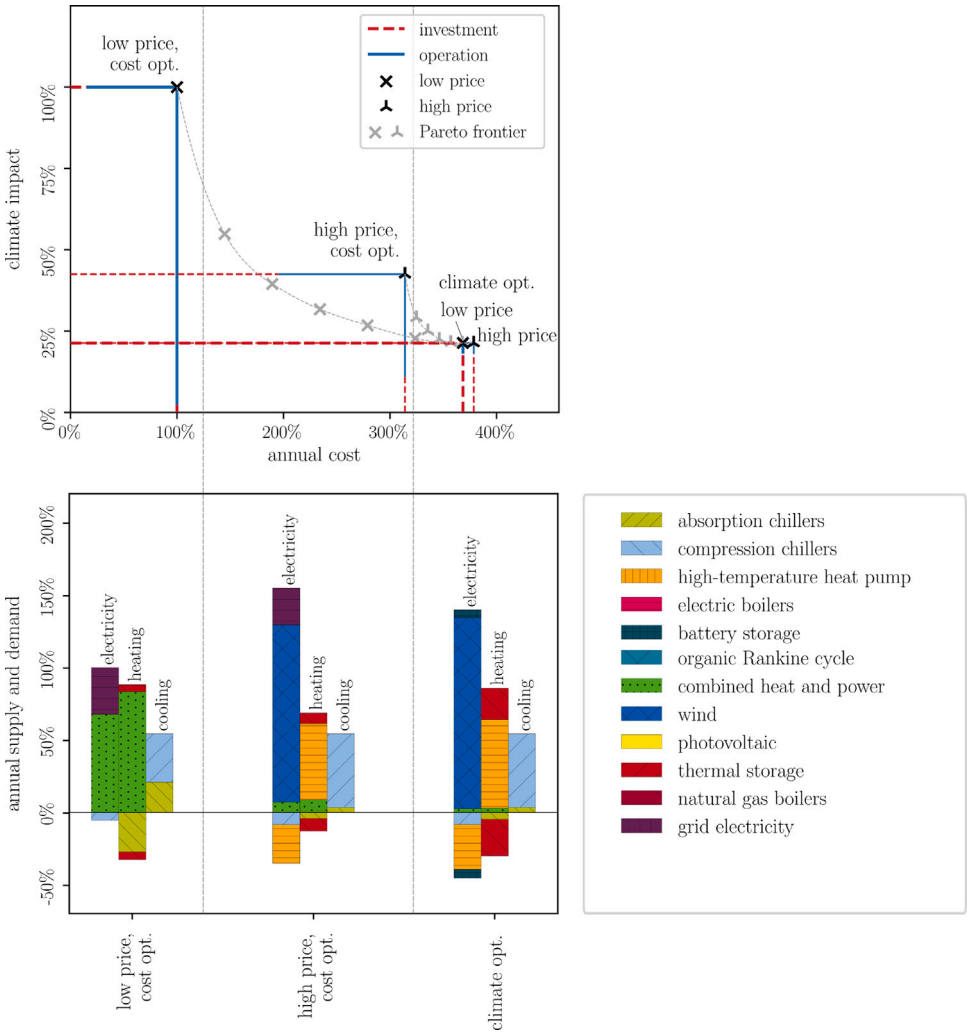

Fig. 4. Annualized cost and climate impact are shown normalized by the respective value in the cost-optimal low-price scenario (top). We further indicate the contribution to costs and climate impact of investment (red, dashed) and operational (blue) phase. Annual electricity, heat, and cooling supply (positive values) and endogenous demand (negative values) for the cost-optimal low and high price scenarios and the climate-optimal case (bottom). All energy flows are normalized by the electricity flow in the low-price scenario. For each cost scenario, we indicate the Pareto frontier between the cost-optimal and climate-optimal case in gray.

absorption chillers are used to maximize the load hours of the CHP by employing heat-based cooling.

In the high-price scenario, electricity is provided mainly by local renewable electricity production via wind turbines, as employing the CHPs is much less economically competitive. CHPs are still utilized but to a much lower share. The heat and cooling supply is largely electrified using the high-temperature heat pump and the compression chillers.

When the climate impact is minimized, the system almost entirely relies on wind electricity. The heat and cooling supply is electrified, and battery and thermal storage are used to decouple electricity supply and demand.

However, in our scenarios, the PTES system as a whole is not used in any scenario: While some components of the PTES system – heat pumps and thermal storage – are used in most systems to couple the electricity and heat sectors, the organic Rankine cycle is never used to provide electricity.

The studied PTES system is outperformed by other flexibility options and, therefore, not employed as a whole to provide electricity flexibly. In our scenarios, using heat to provide heating or cooling is the more viable option than reconversion to electricity.

Still, our case study underlines the need for local electricity production and electrification by sector coupling for both economic and environmental purposes.

4. Conclusions

In this work, we extend SecMOD to a MILP optimization framework to consider the optimal design and operation of industrial energy systems. Based on a user-defined superstructure, the MILP extension takes into account the sizing of discrete production and storage components, including their part-load behavior. For a holistic assessment of the considered system, the framework includes a life-cycle assessment in addition to an economic assessment. In this context, both the construction and operational impacts are considered. A flexible objective function allows for the multi-criteria optimization of the system to evaluate the trade-offs between different environmental impacts and costs. Hence, the modular structure of the extended framework allows for optimizing and analyzing systems with regard to various scopes and aspects. As an important tool for the holistic assessment of industrial energy systems, we publish the extended SecMOD MILP framework open-source under https://git-ce.rwth-aachen.de/ltt/secmod-milp. Additionally, we include a minimal example.

We use SecMOD MILP for a holistic design optimization of an industrial energy system. Further, we demonstrate the framework's capabilities and discuss trade-offs for the system design in two scenarios with varying energy prices under an economic and environmental objective. The results of our case study confirm that sector coupling

and energy storage are essential for industrial decarbonization and are economically and environmentally competitive. Regarding pumped-thermal energy storage to enhance flexibility, we find that the heat pump and thermal storage of the PTES system are economically and environmentally viable in most scenarios. However, reconversion to electricity is neither economically nor environmentally competitive for the studied system. However, reconversion to electricity could be economically and environmentally competitive in another system setup, where fewer alternative routes for decarbonization and electrification exist. For example, Tillmanns et al. (2022) discuss the potential of PTES in more detail. PTES is still under development, and thus, significant improvements regarding efficiency and costs are expected (Olympios et al., 2021). A promising approach to decrease PTES cost is the reuse of existing equipment from discontinued coal-fired power plants for the reconversion to electricity (Steinmann et al., 2020). Overall, the economic and environmental competitiveness depends on various factors — the most significant factors are the applicability of alternative components and the environmental and economic performance (e.g., costs, longevity, and conversion efficiency) of pumped-thermal energy storage compared to alternative technologies.

We hope that our framework can contribute to understanding trade-offs in industrial energy systems and hence aids in realizing environmental improvements that can be achieved cost-efficiently.

Nomenclature

Symbol	Explanation
Sets	
B	Products
C^{prod}	Production components
C^{stor}	Storage components
T	Time steps
IMP	Impact categories
S	Part-load segments
Variables	
$P_c^{\text{prod,nom}}$	Production capacity
$P_c^{\text{stor,nom}}$	Storage capacity
$P_{b,c,t}^{\text{prod}}$	Production/consumption of production component
$P_{c,s,t}^{\text{prod,load}}$	Load of production component
$P_{b,c,t}^{\text{stor,load,in}}$	Charging amount of storage component
$P_{b,c,t}^{\text{stor,load,out}}$	Discharging amount of storage component
$P_{b,t}^{\text{buy}}$	Sale of products
$P_{b,t}^{\text{sell}}$	Purchase of products
$\tilde{P}_{c,s,t}^{\text{prod,nom}}$	Auxiliary capacity of production component
$SL_{c,t}$	Storage level
$Z_{c,s,t}^{\text{prod,part}}$	Binary variable for part-load behavior of production component
$Z_c^{\text{stor,exist}}$	Binary variable for existence of storage component
$CAPEX_{imp}$	Annualized capital expenditures
$OPEX_{imp}^{\text{prod}}$	Operational expenditures of production components
$OPEX_{imp}^{\text{stor}}$	Operational expenditures of storage components
$OPEX_{imp}^{\text{exchange}}$	Operational expenditures for purchase and sale of products
Parameters	
$k_{c,imp}^{\text{inv,prod}}$	Specific investment costs for production components
$k_{c,imp}^{\text{inv,stor}}$	Specific investment costs for storage components
$k_{c,imp}^{\text{op,prod}}$	Specific operating costs for production components
$k_{c,imp}^{\text{op,stor}}$	Specific operating costs for storage components
$k_{b,t,imp}^{\text{buy}}$	Specific costs to buy products
$k_{b,t,imp}^{\text{sell}}$	Specific costs to sell products
pvf_c	Present value annuity factor
Δt_t	Time step duration
$capex_{imp}^{\text{lim}}$	Capital expenditures limit
$opex_{imp}^{\text{lim}}$	Operational expenditures limit
$totex_{imp}^{\text{lim}}$	Total expenditures limit
$d_{b,t}$	Product demand
$cap_c^{\text{prod,max}}$	Maximal possible production capacity
$cap_c^{\text{prod,min}}$	Minimal possible production capacity
$cap_c^{\text{stor,max}}$	Maximal possible storage capacity
$cap_c^{\text{stor,min}}$	Minimal possible storage capacity
$\theta_{b,c,s}$	Constant part of product ratio matrix
$\dot{\theta}_{b,c,s}$	Linear part of product ratio matrix
$\underline{rl}_{c,s}$	Minimum relative load
$\overline{rl}_{c,s}$	Maximum relative load
$av_{c,t}$	Relative availability
$sl_c^{\text{stor,min}}$	Minimal relative storage level
$\eta_c^{\text{stor,loss}}$	Relative storage efficiency
$\eta_{b,c}^{\text{stor,in}}$	Charging efficiency
$\eta_{b,c}^{\text{stor,out}}$	Discharging efficiency
$pcr_{b,c}^{\text{stor}}$	Power-to-capacity ratio

CRediT authorship contribution statement

Christiane Reinert: Writing – original draft, Conceptualization, Methodology, Investigation, Visualization, Data curation, Project administration. **Niklas Nolzen:** Writing – original draft, Conceptualization, Methodology, Software, Investigation, Project administration. **Julia Frohmann:** Investigation, Visualization, Data curation. **Dominik Tillmanns:** Investigation, Data curation, Writing – review & editing. **André Bardow:** Writing – review & editing, Conceptualization, Methodology, Supervision, Resources, Funding acquisition.

Declaration of competing interest

The authors declare that they have no known competing financial interests or personal relationships that could have appeared to influence the work reported in this paper.

Data availability

The data analyzed in this study is subject to the following licenses/restrictions: The MILP framework code is published in a Git repository: https://git-ce.rwth-aachen.de/ltt/secmod-milp. While our code is available under an MIT license, the datasets we used as a case study partly require a separate license. Therefore, all proprietary data was replaced in the exemplary case study provided with our framework. Further inquiries can be directed to the corresponding author. Please note that the Gurobi solver and the ecoinvent data used in our case study require a separate license. Requests to access the ecoinvent database should be directed to Ecoinvent, https://ecoinvent.org/.

Acknowledgments

CR thanks the Ministry of Economics, Innovation, Digitalization and Energy of North-Rhine Westphalia (Grant number: EFO 0001G). NN thanks the German Federal Ministry of Economic Affairs and Energy (Grant number: 03EI1015A). This work was partly sponsored by the Swiss Federal Office of Energy's "SWEET" programme and performed in the "PATHFNDR" consortium. The support is gratefully acknowledged. The authors thank Frederike Kuperjans for her contribution to the case study.

Appendix A. Supplementary data

Supplementary material related to this article can be found online at https://doi.org/10.1016/j.compchemeng.2023.108176.

References

Andiappan, V., 2017. State-Of-The-Art Review of Mathematical Optimisation Approaches for Synthesis of Energy Systems. Process Integr. Optim. Sustain. 1 (3), 165–188. http://dx.doi.org/10.1007/s41660-017-0013-2.

Baumgärtner, N., Bahl, B., Hennen, M., Bardow, A., 2019. RiSES3: Rigorous Synthesis of Energy Supply and Storage Systems via time-series relaxation and aggregation. Comput. Chem. Eng. 127, 127–139. http://dx.doi.org/10.1016/j.compchemeng.2019.02.006.

Baumgärtner, N., Deutz, S., Reinert, C., Nolzen, N., Kuepper, E., Hennen, M., Hollermann, D., Bardow, A., 2021. Life-Cycle Assessment of Sector-Coupled National Energy Systems: Environmental Impacts of Electricity, Heat, and Transportation in Germany Till 2050. Front. Energy Res. 9, 1–13. http://dx.doi.org/10.3389/fenrg.2021.621502.

BDEW, 2022. Strompreisanalyse Januar 2022. Haushalte und Industrie (in German). https://www.bdew.de/media/documents/220124_BDEW-Strompreisanalyse_Januar_2022_24.01.2022_final.pdf, (Accessed on 22.09.2022).

Broverman, S.A., 2017. Mathematics of Investment and Credit, Seventh Ed. ACTEX Learning, New Hartford CT.

Brown, T., Hörsch, J., Schlachtberger, D., 2018. PyPSA: Python for Power System Analysis. J. Open Res. Softw. 6, 1–15. http://dx.doi.org/10.5334/jors.188.

Cook, J., Di Martino, M., Allen, R.C., Pistikopoulos, E.N., Avraamidou, S., 2022. A decision-making framework for the optimal design of renewable energy systems under energy-water-land nexus considerations. Sci. Total Environ. 827, 154185. http://dx.doi.org/10.1016/j.scitotenv.2022.154185.

Dumont, O., Frate, G.F., Pillai, A., Lecompte, S., De Paepe, M., Lemort, V., 2020. Carnot battery technology: A state-of-the-art review. J. Energy Storage 32, 101756. http://dx.doi.org/10.1016/j.est.2020.101756.

EEX Market Data Services, 2022. Spot market data, Natural gas market. https://www.powernext.com/spot-market-data, (Accessed on 22.09.2022).

Fleschutz, M., Bohlayer, M., Braun, M., Murphy, M.D., 2022. Demand Response Analysis Framework (DRAF): An Open-Source Multi-Objective Decision Support Tool for Decarbonizing Local Multi-Energy Systems. Sustainability 14 (13), http://dx.doi.org/10.3390/su14138025.

Gerber, L., Fazlollahi, S., Maréchal, F., 2013. A systematic methodology for the environomic design and synthesis of energy systems combining process integration, Life Cycle Assessment and industrial ecology. Comput. Chem. Eng. 59, 2–16. http://dx.doi.org/10.1016/j.compchemeng.2013.05.025, Selected papers from ESCAPE-22 (European Symposium on Computer Aided Process Engineering - 22), 17-20 June 2012, London, UK.

Glover, F., 1975. Improved Linear Integer Programming Formulations of Nonlinear Integer Problems. Manage. Sci. 22 (4), 455–460.

Guelpa, E., Bischi, A., Verda, V., Chertkov, M., Lund, H., 2019. Towards future infrastructures for sustainable multi-energy systems: A review. Energy 184, 2–21. http://dx.doi.org/10.1016/j.energy.2019.05.057.

Halffmann, P., Schäfer, L.E., Dächert, K., Klamroth, K., Ruzika, S., 2022. Exact algorithms for multiobjective linear optimization problems with integer variables: A state of the art survey. J. Multi-Criteria Decis. Anal. 29 (5–6), 341–363. http://dx.doi.org/10.1002/mcda.1780.

Hilpert, S., Kaldemeyer, C., Krien, U., Günther, S., Wingenbach, C., Plessmann, G., 2018. The Open Energy Modelling Framework (oemof) - A new approach to facilitate open science in energy system modelling. Energy Strategy Rev. 22, 16–25. http://dx.doi.org/10.1016/j.esr.2018.07.001.

Hoettecke, L., Schuetz, T., Thiem, S., Niessen, S., 2022. Technology pathways for industrial cogeneration systems: Optimal investment planning considering long-term trends. Appl. Energy 324, 119675. http://dx.doi.org/10.1016/j.apenergy.2022.119675.

Hugo, A., Pistikopoulos, E., 2005. Environmentally conscious long-range planning and design of supply chain networks. J. Clean. Prod. 13 (15), 1471–1491. http://dx.doi.org/10.1016/j.jclepro.2005.04.011, Recent advances in industrial process optimisation.

International Energy Agency, 2021. Renewables 2021: Analysis and forecast to 2026.

ISO, 2020a. Environmental management - Life Cycle Assessment - Principles and framework. EN ISO 14040:2006 + AMD 1:2020, International Organization for Standardization, Brussels, Belgium.

ISO, 2020b. Environmental management - Life Cycle Assessment - Requirements and guidelines. EN ISO 14044:2006+AMD 1:2017+AMD 2:2020, Standard, International Organization for Standardization, Brussels, Belgium.

Joint Research Center, 2010. International Reference Life Cycle Data System (ILCD) Handbook: General guide for Life Cycle Assessment. Detailed guidance. First edition 2010.

Kämper, A., Holtwerth, A., Leenders, L., Bardow, A., 2021a. AutoMoG 3D: Automated Data-Driven Model Generation of Multi-Energy Systems Using Hinging Hyperplanes. Front. Energy Res. 9, 719658. http://dx.doi.org/10.3389/fenrg.2021.719658.

Kämper, A., Leenders, L., Bahl, B., Bardow, A., 2021b. AutoMoG: Automated data-driven Model Generation of multi-energy systems using piecewise-linear regression. Comput. Chem. Eng. 145, 107162. http://dx.doi.org/10.1016/j.compchemeng.2020.107162.

Kantor, I., Robineau, J.-L., Bütün, H., Maréchal, F., 2020. A Mixed-Integer Linear Programming Formulation for Optimizing Multi-Scale Material and Energy Integration. Front. Energy Res. 8, 1–20. http://dx.doi.org/10.3389/fenrg.2020.00049.

Kotzur, L., Markewitz, P., Robinius, M., Stolten, D., 2018. Impact of different time series aggregation methods on optimal energy system design. Renew. Energy 117 (4), 474–487. http://dx.doi.org/10.1016/j.renene.2017.10.017.

Kotzur, L., Nolting, L., Hoffmann, M., Groß, T., Smolenko, A., Priesmann, J., Büsing, H., Beer, R., Kullmann, F., Singh, B., Praktiknjo, A., Stolten, D., Robinius, M., 2021. A modeler's guide to handle complexity in energy systems optimization. Adv. Appl. Energy 4, 100063. http://dx.doi.org/10.1016/j.adapen.2021.100063.

Langiu, M., Shu, D.Y., Baader, F.J., Hering, D., Bau, U., Xhonneux, A., Müller, D., Bardow, A., Mitsos, A., Dahmen, M., 2021. COMANDO: A Next-Generation Open-Source Framework for Energy Systems Optimization. Comput. Chem. Eng. 152, 107366. http://dx.doi.org/10.1016/j.compchemeng.2021.107366.

Limpens, G., Moret, S., Jeanmart, H., Maréchal, F., 2019. EnergyScope TD: A novel open-source model for regional energy systems. Appl. Energy 255, 113729. http://dx.doi.org/10.1016/j.apenergy.2019.113729.

Lopion, P., Markewitz, P., Robinius, M., Stolten, D., 2018. A review of current challenges and trends in energy systems modeling. Renew. Sustain. Energy Rev. 96, 156–166. http://dx.doi.org/10.1016/j.rser.2018.07.045.

Mavrotas, G., 2009. Effective implementation of the ϵ-constraint method in Multi-Objective Mathematical Programming problems. Appl. Math. Comput. 213 (2), 455–465. http://dx.doi.org/10.1016/j.amc.2009.03.037.

Mitsos, A., Asprion, N., Floudas, C.A., Bortz, M., Baldea, M., Bonvin, D., Caspari, A., Schäfer, P., 2018. Challenges in process optimization for new feedstocks and energy sources. Comput. Chem. Eng. 113, 209–221. http://dx.doi.org/10.1016/j.compchemeng.2018.03.013.

Olympios, A.V., McTigue, J.D., Farres-Antunez, P., Tafone, A., Romagnoli, A., Li, Y., Ding, Y., Steinmann, W.-D., Wang, L., Chen, H., Markides, C.N., 2021. Progress and prospects of thermo-mechanical energy storage — a critical review. Progr. Energy 3 (2), 022001. http://dx.doi.org/10.1088/2516-1083/abdbba.

Petchrompo, S., Coit, D.W., Brintrup, A., Wannakrairot, A., Parlikad, A.K., 2022. A review of Pareto pruning methods for multi-objective optimization. Comput. Ind. Eng. 167, 108022. http://dx.doi.org/10.1016/j.cie.2022.108022.

Pfenninger, S., Hirth, L., Schlecht, I., Schmid, E., Wiese, F., Brown, T., Davis, C., Gidden, M., Heinrichs, H., Heuberger, C., Hilpert, S., Krien, U., Matke, C., Nebel, A., Morrison, R., Müller, B., Pleßmann, G., Reeg, M., Richstein, J.C., Shivakumar, A., Staffell, I., Tröndle, T., Wingenbach, C., 2018. Opening the black box of energy modelling: Strategies and lessons learned. Energy Strategy Rev. 19, 63–71. http://dx.doi.org/10.1016/j.esr.2017.12.002.

Rauner, S., Budzinski, M., 2017. Holistic energy system modeling combining multi-objective optimization and life cycle assessment. Environ. Res. Lett. 12 (12), 124005. http://dx.doi.org/10.1088/1748-9326/aa914d.

Reinert, C., Deutz, S., Minten, H., Dörpinghaus, L., von Pfingsten, S., Baumgärtner, N., Bardow, A., 2021. Environmental impacts of the future German energy system from integrated energy systems optimization and dynamic life cycle assessment. Comput. Chem. Eng. 153, 107406. http://dx.doi.org/10.1016/j.compchemeng.2021.107406.

Reinert, C., Schellhas, L., Frohmann, J., Nolzen, N., Tillmanns, D., Baumgärtner, N., Deutz, S., Bardow, A., 2022a. Combining optimization and life cycle assessment: Design of low-carbon multi-energy systems in the SecMOD framework. In: Montastruc, L., Negny, S. (Eds.), 32nd European Symposium on Computer Aided Process Engineering. In: Computer Aided Chemical Engineering, Vol. 51, Elsevier, pp. 1201–1206. http://dx.doi.org/10.1016/B978-0-323-95879-0.50201-0.

Reinert, C., Schellhas, L., Mannhardt, J., Shu, D.Y., Kämper, A., Baumgärtner, N., Deutz, S., Bardow, A., 2022b. SecMOD: An Open-Source Modular Framework Combining Multi-Sector System Optimization and Life-Cycle Assessment. Front. Energy Res. 10, 1–17. http://dx.doi.org/10.3389/fenrg.2022.884525.

Ringkjøb, H.-K., Haugan, P.M., Solbrekke, I.M., 2018. A review of modelling tools for energy and electricity systems with large shares of variable renewables. Renew. Sustain. Energy Revi. 96, 440–459. http://dx.doi.org/10.1016/j.rser.2018.08.002.

Sánchez Diéguez, M., Fattahi, A., Sijm, J., Morales España, G., Faaij, A., 2022. Linear programing formulation of a high temporal and technological resolution integrated energy system model for the energy transition. MethodsX 9, 101732. http://dx.doi.org/10.1016/j.mex.2022.101732.

Steinmann, W.-D., Jockenhöfer, H., Bauer, D., 2020. Thermodynamic Analysis of High-Temperature Carnot Battery Concepts. Energy Technol. 8 (3), 1900895. http://dx.doi.org/10.1002/ente.201900895.

Stoppato, A., Benato, A., 2020. Life Cycle Assessment of a Commercially Available Organic Rankine Cycle Unit Coupled with a Biomass Boiler. Energies 13 (7), 1835. http://dx.doi.org/10.3390/en13071835.

Tartière, T., Astolfi, M., 2017. A World Overview of the Organic Rankine Cycle Market. Energy Procedia 129, 2–9. http://dx.doi.org/10.1016/j.egypro.2017.09.159.

Tillmanns, D., Pell, D., Schilling, J., Bardow, A., 2022. The Thermo-Economic Potential of ORC-Based Pumped-Thermal Electricity Storage: Insights from the Integrated Design of Processes and Working Fluids. Energy Technol. 10, 2200182. http://dx.doi.org/10.1002/ente.202200182.

TOP-Energy, 2022. TOP-Energy 3.1 Ihre Softwarlösung zur Optimierung von Energiesystemen. https://www.top-energy.de.

Voll, P., Klaffke, C., Hennen, M., Bardow, A., 2013. Automated superstructure-based synthesis and optimization of distributed energy supply systems. Energy 50, 374–388. http://dx.doi.org/10.1016/j.energy.2012.10.045.

Wernet, G., Bauer, C., Steubing, B., Reinhard, J., Moreno-Ruiz, E., Weidema, B., 2016. The ecoinvent database version 3 (part I): overview and methodology. Int. J. Life Cycle Assess. 21, 1218–1230. http://dx.doi.org/10.1007/s11367-016-1087-8.

Wirtz, M., Hahn, M., Schreiber, T., Müller, D., 2021. Design optimization of multi-energy systems using mixed-integer linear programming: Which model complexity and level of detail is sufficient? Energy Convers. Manage. 240, 114249. http://dx.doi.org/10.1016/j.enconman.2021.114249.